

A Scaling Law to Predict the Finite-Length Performance of Spatially-Coupled LDPC Codes

Pablo M. Olmos and Rüdiger Urbanke

Abstract—Spatially-coupled LDPC codes are known to have excellent asymptotic properties. Much less is known regarding their finite-length performance. We propose a scaling law to predict the error probability of finite-length spatially coupled ensembles when transmission takes place over the binary erasure channel. We discuss how the parameters of the scaling law are connected to fundamental quantities appearing in the asymptotic analysis of these ensembles and we verify that the predictions of the scaling law fit well to the data derived from simulations over a wide range of parameters. The ultimate goal of this line of research is to develop analytic tools for the design of good finite-length error correcting codes.

Index Terms—codes on graphs, spatially coupled LDPC codes, iterative decoding thresholds, finite-length code performance.

I. INTRODUCTION

RECENTLY, it has been proved that spatially coupled low-density parity-check (SC-LDPC) codes can be designed to achieve capacity over general binary-input memoryless output-symmetric (BMS) channels under belief propagation (BP) decoding [1]. A SC-LDPC ensemble is constructed by coupling a chain of L (l, r) -regular LDPC block codes, each one of length M bits, together with appropriate boundary conditions. The resulting graph typically has a so-called “structured irregularity”, where parity check nodes located at the ends of the chain are connected to a smaller number of variable nodes than those in the middle [2]. As a result, the nodes at the ends of the graph form strong sub-codes and the resulting reliable information generated there during BP decoding propagates in a wave-like fashion from the ends towards the center. When M tends to infinity and L is taken large, SC-LDPC ensembles exhibit a BP threshold arbitrarily close to the maximum-a-posteriori (MAP) threshold of the underlying (l, r) -regular LDPC block ensemble [1], [2].

It is probably fair to state that the asymptotic performance of SC-LDPC codes is well understood. Much less is known about their finite-length behavior [3]. The finite-length analysis of a particular SC-LDPC ensemble consists of relating the BP block error probability to the code parameters, namely the degrees (l, r) , the chain length L , the coupling pattern,

and the code length $n = ML$. In this work, we focus on the finite-length decoding properties of a specific class of SC-LDPC codes, usually referred to as LPDC convolutional (LDPCC) codes [2], [4], when they are used for transmission over the binary erasure channel (BEC). LDPCC codes are characterized by a regular coupling pattern, which makes them particularly suited for practical implementation [5] and for efficient windowed decoding [6]. It is conjectured that LDPCC ensembles achieve channel capacity of BMS channels [3], [2].

In [7] we provided a first description of the scaling behavior of finite-length LDPCC ensembles using an extensive set of simulations. Let us recall some basic observations from [7]. First, if we increase the chain length L for a fixed M then the performance degrades. The longer the chain, the more time the “decoding wave” needs to sweep over the whole chain, since the speed of the decoding wave only depends on the channel parameter but not on the length of the chain [1]. Therefore, there is a larger chance that the decoding wave gets “stuck,” i.e., that the decoding process fails. Second, and perhaps more surprisingly and practically important, this increase in the error probability when L increases is small and it can be easily compensated by a slight increase in M . Indeed, based on simulations and some simple back of the envelope calculations, it was observed in [7] that L can increase at a speed almost exponentially in M in order to maintain a constant error probability. In [7] these conclusions were based, besides on simulations, on calculations in the so-called error-floor regime, i.e., by counting the number of low-weight codewords as a function of L and M . No closed-form expression was provided to evaluate the error probability in the range of most interest, namely when we consider coupled codes above the BP threshold of (l, r) -regular LDPC code.

In the present work we extend to convolutional LDPC ensembles the methodology proposed in [8] to analyze finite-length uncoupled LDPC ensembles. For the BEC, the workings of the BP decoder can be cast in an alternative formulation, namely as peeling decoding (PD) [9]. In this formulation, any time the value of a variable node is determined, this variable node and all attached edges are removed from the graph. The analysis then consists of studying the statistical evolution of the residual graph as a function of time [10]. More precisely, for the analysis it suffices to track the *average* evolution of the graph since it can be shown that the evolution of most decoding instances stay close to this average. [9]. If in addition we determine the variance around this average, then we can predict the decoding block error probability, since errors in this framework correspond to deviations from the expected behavior beyond a certain threshold.

Pablo M. Olmos is with the Dept. Teoría de la Señal y Comunicaciones, Universidad Carlos III de Madrid, Avda. de la Universidad 30, 28911, Leganés (Madrid), Spain. E-mail: olmos@tsc.uc3m.es

Rüdiger Urbanke is with the School of Computer and Communication Sciences, École Polytechnique Fédérale de Lausanne, Switzerland. E-mail: ruediger.urbanke@epfl.ch

This work was supported by the European project STAMINA, 265496, and by Spanish government MEC TEC2009-14504-C02-01 and TEC2012-38800-C03-01 and Consolider-Ingenio 2010 CSD2008-00010).

This work was presented in part at the IEEE Information Theory Workshop, Sevilla, Spain, Sept. 2013.

We derive the system of differential equations that determines the mean and covariance of the LDPC graph evolution over the PD process. As proved in [8] in the context of LDPC block codes, the residual graph degree distribution is a random process that tends (in M) to be Gaussian and the mean and covariance matrix are given by the solution of the derived system of differential equations. We also show that the process covariance between two different decoding time instants τ and ζ decays exponentially with $|\tau - \zeta|$ and that the rate of decay is controlled by a parameter related to the LDPC coupling pattern.

For uncoupled regular LDPC ensembles, the PD error probability is dominated by the behavior of the graph evolution at typically a single “critical” time during the decoding process [11]. For LDPC codes, to the contrary, we show that the decoder might fail roughly with uniform probability throughout the whole decoding process. In addition, we show that the dominant statistics of the residual graph evolution process fit those of an appropriately chosen Ornstein-Uhlenbeck (OU) process [12] and, furthermore, that the OU process is the only possible underlying model based on the two first moments of the graph evolution process. OU processes have been widely studied and used in diverse areas of applied mathematics like biological modeling [13], [14], mathematical finance [15], [16] and statistical physics [17].

By using known results and expressions for the OU survival time probability density function (pdf) [18], [17], [19], we derive a closed-form expression to estimate the error probability of LDPC ensembles. We illustrate the accuracy of the obtained scaling law by comparing its predictions with error probability curves derived via simulations. As we will discuss, there is a very good fit over a wide range of parameters. These simulation results also confirm that the model underlying our derivations, namely the assumption that the decoding path is modeled by an OU process, is a very good fit and holds out the hope that this assumption can eventually be brought on a rigorous analytic basis.

Further, the presented closed-form scaling law is consistent with the behavior observed by simulation in [7], explaining the underlying scaling between L , M and the LDPC error probability. In particular, the scaling law proposed for LDPC codes reflects that the degradation in performance caused by an exponential increase in the chain length L can be compensated by a slight increase in M . We believe that the results presented in this paper contribute to a better understanding of finite-length SC-LDPC codes and, in particular, that the proposed scaling law constitutes a useful engineering tool for code design.

In Section II we review the construction of convolutional LDPC ensembles. In Section III, we derive the differential equations that describe the expected LDPC graph evolution during PD. Graph covariance evolution is discussed in Section IV. In Section V, we present a scaling law to predict the LDPC block error performance based on closed-form expressions for the OU process survival probability. Finally, we provide some concluding remarks in Section VI, including potential future lines of research on this topic.

II. CONVOLUTIONAL LDPC ENSEMBLES

Let us now describe and define the ensemble that we consider.

A. Basic construction

Consider a set of L (l, r) -regular LDPC codes, where l is the variable-node degree and $r \geq l$ is the check-node degree. Further, each code has length M , i.e., there are M variable nodes/bits, each of degree l and there are $\frac{l}{r}M$ (assume it to be integer) check nodes, each of degree r . Place these L (l, r) -regular codes at “positions” indexed from 1 to L . In order to generate a spatially-coupled code we will now let these L codes “interact” by ensuring that edges do not only appear between variable and check nodes at the same position, but are “spread out” in a certain neighborhood. For the purpose of this paper we will assume a very regular coupling pattern. We refer to this ensemble as the (r, l, L) ensemble.

More precisely, recall that variable nodes are placed at positions 1 to L (always M at each position). Consider a variable node at position i , $1 \leq i \leq L$. By assumption this variable node has degree l . For each j , $j = 0, \dots, l-1$, take one of these edges and connect it to a check node at position $i+j$. Note that in this model check nodes are in fact placed at positions i , $1 \leq i \leq D = L + l - 1$, i.e., there are $l-1$ extra positions of check nodes compared to variable nodes. For the positions j , $l \leq j \leq L$, there are exactly $Ml = \frac{l}{r}Mr$ edges that go to check nodes at these positions. Each check node has degree r . To connect these edges to these check nodes label the edges in an arbitrary but fixed manner and do the same for all check node sockets. Now pick a random permutation on Ml elements and connect edges to sockets according to this permutation. For the positions $l-j$ and $L+j$, $1 \leq j \leq l-1$, the number of edges connecting to check nodes at these positions is only $M(l-j)$ but there are still Ml check node sockets to which we can potentially connect. For these positions we proceed in a similar manner by picking a random permutation on Ml elements but only the first $M(l-j)$ correspond to real edges, whereas the remaining sockets remain empty. In this way check nodes in these positions have maximum degree r and their actual degree follows a Binomial distribution.

Some thought shows that the (l, r, L) design rate a function of l , r and L is

$$r = 1 - \frac{l}{r} \frac{L + 2 \sum_{j=1}^{(l-1)} 1 - \left(\frac{l-j}{l}\right)^r}{L}. \quad (1)$$

This tends to $1 - l/r$, the rate of the uncoupled (l, r) -regular LDPC block code, when $L \rightarrow \infty$.

B. Some further remarks on the construction

A few further remarks on this construction might be helpful. As we have seen, variable nodes have degree l . Check nodes have degree r (in the range $l \leq i \leq L$, and a Binomial degree distribution at the boundary) Further, if we consider a random edge connected to a check node at position i , $l-1 \leq i \leq L$, then it is connected to a variable node at position $i-j$ with

j uniformly chosen in $[0, l - 1]$ and within this position the variable node is chosen uniformly at random.

The ensemble as defined above is convenient for the purpose of analysis. It is not necessarily the most convenient in terms of implementation or the best in terms of performance. In [2], a protograph-based construction of an (l, r, L) ensemble was introduced. In this construction, with probability one each check node at position j has exactly $\frac{r}{l}$ edges (assume it to be integer) connected to variables at position i , for $i = j, j - 1, \dots, j - l + 1$. Simulation results show that this ensemble has a very good performance and also this ensemble seems well suited for implementations [20], [21]. The same analysis that we perform on our ensemble could in principle be done for this protograph ensemble but the necessary calculations are more involved.

In the rest of the paper we restrict to the random construction of the (l, r, L) ensemble introduced above. Simulation results suggest that the form of the scaling law we derive also applies to protograph-based LPDCC codes if the scaling parameters are adjusted appropriately [22].

III. PEELING DECODING AND EXPECTED GRAPH EVOLUTION

Consider transmission over the binary erasure channel (BEC) and decoding using the peeling decoder (PD) [11]. At each step, the PD removes one degree-one check node and its connected variable node, as well as all edges connected to these two nodes. In [9], it is shown that if we apply the PD to elements of an LDPC ensemble, then the sequence of graphs which are generated during the decoding process follows a typical path or expected evolution. This expected path in terms can be computed by solving a system of coupled differential equations. And in turn, from the expected path one can determine the asymptotic performance, and in particular the threshold

In [8], *scaling laws* (SLs) were proposed to accurately predict the BP finite-length performance in the waterfall region and it was also shown how to compute the parameters of the scaling law from the degree distribution of the ensemble. More precisely, the four most important parameters of the scaling law are (i) the threshold, (ii) the “critical time(s)” of the process, i.e., the time at which the expected number of degree-one check nodes reaches a local minimum, (iii) the expected number of degree-one check nodes at these critical times, and (iv) the variance of this number at the critical time(s). The first three parameters can be determined by looking at the LDPC expected path. To determine the fourth parameter a further system of differential equations, dubbed covariance evolution in [8] has to be solved. If we assume that there is only a single critical time, then the error probability can be estimated from the relationship between the expected number of degree-one check nodes at the critical time and the variance of the same quantity at this point in time.

In order to derive a scaling law, we apply a similar line of reasoning to the (l, r, L) ensemble. But as we will see, the error mechanism is slightly different in this case. The main difference to the case of standard (uncoupled) LDPC

ensembles is that for coupled ensembles there is no particular “critical” time but that for coupled ensembles the decoder might fail roughly with uniform probability throughout the whole decoding process (this ignores the initial and final phase of the decoder). In Section III-B, we compute the (l, r, L) expected graph evolution and discuss the first three scaling parameters (i)-(iii). In Section IV, we derive the covariance evolution system of differential equations and compute the variance scaling parameters.

A. Description of ensemble in terms of degree distribution

Our aim is to describe the evolution of the ensemble during the decoding process as a function of time. We do this by describing how the *degree distribution* (DD) evolves. In the sequel we will denote time by ℓ if we measure time in discrete steps and by τ once we rescale time to pass to the continuous limit in order to write down a differential equation, where $\tau = \ell/M$.

At time ℓ , $\ell \in \mathbb{N}$, let $R_{j,u}(\ell)$ be the number of edges that are connected to check nodes of degree j placed at position u and let $E_u(\ell)$ be the total number of edges connected to check nodes at position u . Thus,

$$E_u(\ell) = \sum_{j=1}^r R_{j,u}(\ell). \quad (2)$$

Note that for our case all variable nodes are of degree l . It suffices therefore to know the number of variable nodes per position. Let this number be denoted as $V_u(\ell)$. Then

$$l \sum_{u=1}^D V_u(\ell) = \sum_{u=1}^D E_u(\ell) = \sum_{u=1}^D \sum_{j=1}^r R_{j,u}(\ell) \doteq E(\ell), \quad (3)$$

where $E(\ell)$ is the total number of edges in the code.

B. (l, r, L) expected graph evolution

Assume that we use samples from the (l, r, L) ensemble to transmit over a BEC with erasure probability ϵ . We initialize the PD by removing from the graph all variable nodes whose value was received through the channel as well as all their edges. At each iteration, the PD then chooses a degree-one check node. This check node is removed along with the connected variable node and all connected edges.

Let $V_u(\ell)$ and $R_{j,u}(\ell)$ be the DD at position u after ℓ PD iterations. Let $\ell = 0$ be the state of the system after the initialization. Then the expected DD at this time is given by

$$\mathbb{E}[V_u(0)] = \epsilon M \mathbb{1}[1 \leq u \leq L], \quad (4)$$

$$\mathbb{E}[R_{j,u}(0)] = j \frac{l}{r} M \sum_{m \geq j} \rho_m \binom{m}{j} \epsilon^j (1 - \epsilon)^{(m-j)} \quad (5)$$

where

$$\rho_m = \binom{r}{m} \left(\frac{d_u}{l}\right)^m \left(1 - \frac{d_u}{l}\right)^{(r-m)} \quad (6)$$

and

$$d_u = \begin{cases} u, & u \leq l-1, \\ l, & l \leq u \leq L, \\ L+l-u, & L+1 \leq u \leq L+l-1, \\ 0, & \text{otherwise.} \end{cases} \quad (7)$$

For the variable nodes the expression is very straightforward. For every position $1 \leq u \leq L$ there are M variable nodes, each of degree l . Each such variable nodes rests in the graph if and only if it was erased during transmission, and the latter happens with probability ϵ .

For check nodes the situation is more complicated. Every check node at position $1 \leq u \leq D$ has r sockets. But there are two mechanisms at work so that not all these sockets are in generally filled. First, towards the boundary, the total number of edges decreases. This is taken into account by the factor d_u/l which is 1 for $l \leq u \leq L$ but strictly smaller at the boundary. Second, as explained in the previous section, before we start the decoding process we only keep those variables (and their attached edges) which were erased in the decoding process.

Let $\mathcal{G}(\tau) = \{\mathcal{G}_{j,u}(\tau)\}$ for $u = 1, \dots, D$ and $j = 1, \dots, r+1$ be the normalized DD at time $\tau \doteq \ell/M$, where

$$\mathcal{G}_{j,u}(\tau) = \begin{cases} r_{j,u}(\tau) & j \in \{1, \dots, r\} \\ v_u(\tau) & j = r+1 \end{cases}, \quad (8)$$

and

$$r_{j,u}(\tau) \doteq \frac{R_{j,u}(\ell)}{M} \quad \text{and} \quad v_u(\tau) \doteq \frac{V_u(\ell)}{M}. \quad (9)$$

$\mathcal{G}(\tau)$ is a random process that constitutes a sufficient statistic to analyze the decoding process of the (l, r, L) ensemble and to predict the error probability. In the following, we refer to it as the residual DD process. In this section we show how to compute $\mathbb{E}[\mathcal{G}(\tau)]$ as a function of time. As shown in [9], [11],

the system of differential equations

$$\frac{\partial \hat{\mathcal{G}}_{j,u}(\tau)}{\partial \tau} = f_{j,u}(\hat{\mathcal{G}}(\tau)) \quad (10)$$

for $u = 1, \dots, D$ and $j = 1, \dots, r+1$, where

$$f_{j,u}(\mathcal{G}(\tau)) \doteq \frac{\mathbb{E} \left[\mathcal{G}_{j,u}(\tau + \frac{1}{M}) - \mathcal{G}_{j,u}(\tau) \mid \mathcal{G}(\tau) \right]}{1/M}, \quad (11)$$

has a unique solution and, further, the solution for the initial conditions $\hat{\mathcal{G}}_{r+1,u}(0) = \mathbb{E}[V_u(0)]/M$ and $\hat{\mathcal{G}}_{j,u}(0) = \mathbb{E}[R_{j,u}(0)]/M$, given in (4) and (5), deviates from the true mean evolution of $\mathcal{G}(\tau)$ by less than M^{-1} . In addition, with probability $1 - \mathcal{O}(e^{-\sqrt{M}})$, any sample of the residual DD process \mathcal{G} deviates from $\hat{\mathcal{G}}$ by less than $M^{-1/6}$ [11]. Consequently, in the limit $M \rightarrow \infty$, samples of the process $\mathcal{G}(\tau)$ closely follow $\hat{\mathcal{G}}(\tau)$.

Note that the function $f_{j,u}(\hat{\mathcal{G}}(\tau))$ represents the ‘‘drift’’ (expected change) in the components of the DD as a result of one decoding step when the DD at time τ is fixed to $\hat{\mathcal{G}}(\tau)$. To evaluate the probability of successful decoding, we have to estimate the survival probability of the random process

$$r_1(\tau) \doteq \sum_{m=1}^D \mathcal{G}_{1,m}(\tau) = \sum_{m=1}^D r_{1,m}(\tau), \quad (12)$$

i.e., we have to determine the probability that this quantity stays strictly positive until the whole graph has been ‘‘peeled’’ off.

The ensemble BP threshold $\epsilon_{(l,r,L)}$ is defined as the maximum ϵ for which the expected evolution of the normalized number of degree-one check nodes in the graph, i.e.,

$$\hat{r}_1(\tau) \doteq \sum_{m=1}^D \hat{\mathcal{G}}_{1,m}(\tau) = \sum_{m=1}^D \hat{r}_{1,m}(\tau), \quad (13)$$

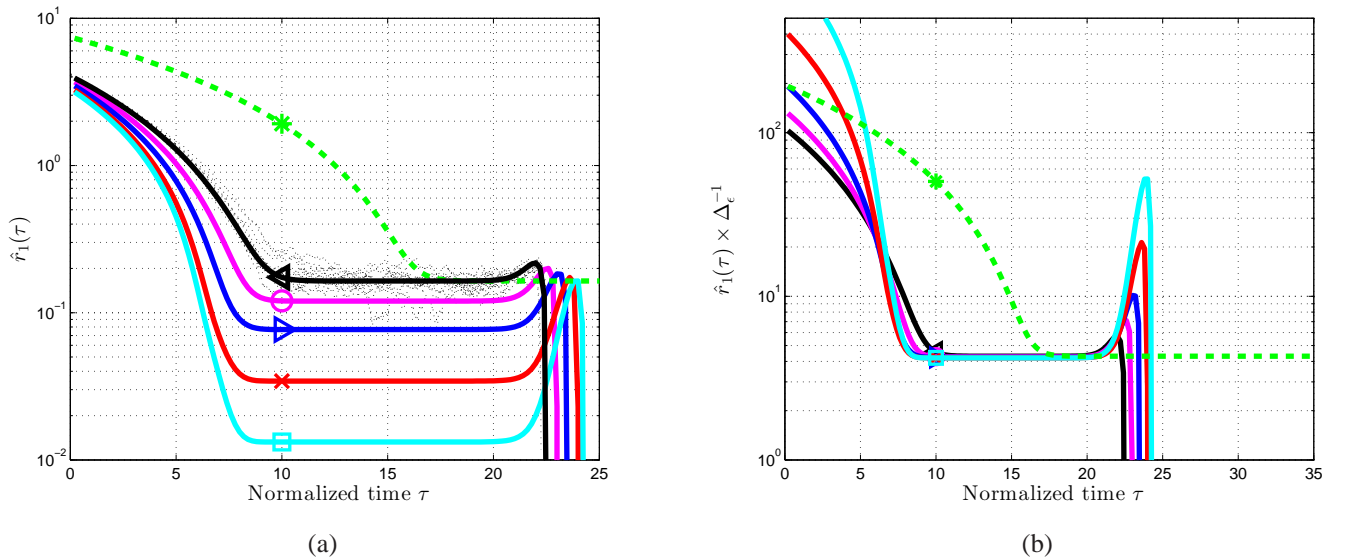


Fig. 1. In (a), we plot the solution of $\hat{r}_1(\tau)$ for the (l, r, L) ensemble with $L = 50$, $l = 3$, $r = 6$ and different ϵ values: 0.45 (\blacktriangleleft), 0.46 (\circ), 0.47 (\blacktriangleright), 0.48 (\times) and 0.485 (\square). For $\epsilon = 0.45$, we have included a set of 10 empirical trajectories computed for $M = 1000$, dotted thin lines. In (b), we normalize the $\hat{r}_1(\tau)$ curves by Δ_ϵ . The dashed line with $*$ marker, shows the solution for the same ensemble with twice the chain length, i.e., $L = 100$, and $\epsilon = 0.45$.

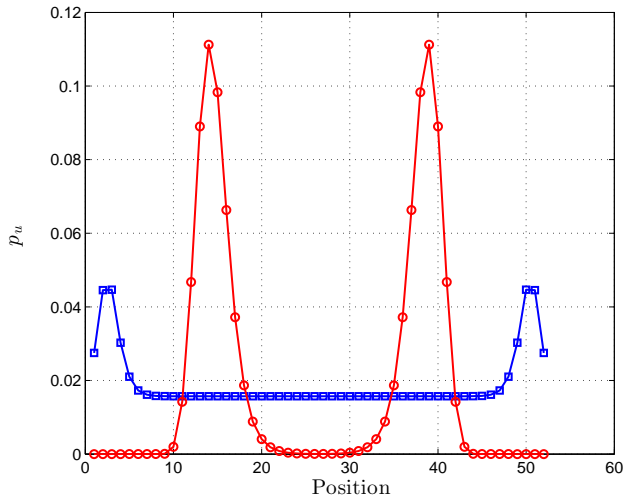


Fig. 2. For a convolutional LDPC code with $L = 50$, $l = 3$, $r = 6$, we plot the $p_u(\tau)$ profile at $\tau = 5$ (\square) and $\tau = 15$ (\circ) for $\epsilon = 0.45$. Note that $\tau = 5$ is a point during the initial phase, whereas $\tau = 15$ is a point during the steady state phase.

is strictly positive for any $\tau \in [0, \epsilon L]$. The details of the computation of the expectations in (11) for the (l, r, L) ensemble can be found in Appendix A.

C. Solution and comparison for different ensembles

In Fig. 1(a), we plot the solution to $\hat{r}_1(\tau)$ for the (l, r, L) ensemble with $L = 50$, $l = 3$ and $r = 6$ for different values of ϵ . The solution to the system in (10) is numerically computed using Euler's method. The curves initially quickly decay from their starting value until they reach a constant value. They then stay at this constant value until the very end of the decoding process. Note that the higher we pick ϵ the closer this constant gets to the zero value. The threshold is that ϵ value where the corresponding constant reaches zero. For $L = 50$, the BP threshold is $\epsilon_{(3,6,L=50)} = 0.48815$ [3], [2]. For the case $\epsilon = 0.45$, we have included a set of 10 simulated decoding trajectories computed for $M = 1000$ bits per position of the code to show that they concentrate around the predicted mean evolution.

Let us discuss these curves in some more detail. These trajectories look quite different from the typical trajectories of uncoupled LDPC ensembles [8]. Let us first look at the initial phase. This initial phase behaves essentially as in the uncoupled case: first, all correctly received variable nodes are removed. Then later on “easy” deductions are being made and they appear more or less uniformly along the chain. These “easy” deductions correspond to degree-one check nodes that are more or less uniformly spread along the length of the chain. In Fig. 1(a) this phase corresponds to the initial decreasing branch. If we are transmitting at a channel value which is strictly above the BP threshold of the uncoupled (l, r) -regular LDPC block ensemble, then this phase ends when the system is roughly in the fixed-point state which the uncoupled ensemble would reach.

The second phase starts at $\tau^* = \tau^*(l, r, L, \epsilon)$, when the positions in the center of the code have run out of degree-one check nodes. This phase corresponds to the “decoding” wave which moves at constant speed throughout the graph [3], [7]. In this phase the degree-one check nodes which are being removed occur mostly around the position where the decoding wave has its rapid rise. Note that in this phase we do not have one critical time point at which the decoder is most likely to stop, but the expected number of degree-one check nodes is essentially a constant throughout this phase. Therefore, we call this the “steady state” phase. Strictly speaking, as pointed out in [3], the evolution is not completely flat but exhibits small wiggles. But these wiggles are extremely small and, further, their amplitude vanish when l is increased. For instance, in the $(l = 3, r = 6, L)$ example illustrated above, the amplitude of the oscillation is 10^{-7} .

Finally, when the two decoding waves starting at the two ends of the chain are meeting in the middle of the chain, a third phase takes over. For properly designed spatially-coupled ensembles it is very unlikely for the decoder to get stuck in either the first or the last phase. We therefore concentrate on the intermediate steady state phase and inquire how we can express the error probability as a function of the behavior of the residual DD process.

Denote by $\hat{r}_1(*)$ the mean value of the fraction of degree-one check nodes during the steady state phase. As expected, $\hat{r}_1(*) \rightarrow 0$ as the channel parameter approaches the BP threshold. Imagine we are exactly at the BP threshold of the (l, r, L) ensemble, i.e. $\epsilon = \epsilon_{(r,l,L)}$, and we slightly reduce ϵ . By simply plotting $\hat{r}_1(\tau)/\Delta_\epsilon$ (see Fig. 1(b)), where $\Delta_\epsilon = \epsilon_{(r,l,L)} - \epsilon$, we observe that, as shown for LDPC block ensembles in [8], a first-order Taylor expansion of $\hat{r}_1(*)$ around $\epsilon_{(r,l,L)}$ provides an accurate approximation to $\hat{r}_1(*)$ as a function of ϵ :

$$\hat{r}_1(*) \approx \gamma \Delta_\epsilon, \quad (14)$$

where $\gamma = \gamma(l, r)$ depends on the regular underlying ensemble. For the $(l = 3, r = 6)$ case, we get $\gamma \approx 4.19$. In Table I, we include the value of γ for different values of l and r as well as the MAP threshold for the underlying LDPC regular code, which represents the BP threshold of the (l, r, L) ensemble in the limit $L \rightarrow \infty$.

l	r	MAP threshold	γ
3	6	0.5445	4.19
4	8	0.4977	4.11
5	10	0.4994	4.04
4	12	0.3302	4.07
5	15	0.3325	4.01
4	6	0.6656	4.09

TABLE I
 γ PARAMETER FOR DIFFERENT (l, r, L) ENSEMBLES.

To better understand the nature of the behavior observed in Fig. 1, consider the expected probability $p_u(\tau)$ that the PD removes a check node from position u at time τ :

$$p_u(\tau) \doteq \frac{\hat{r}_{1,u}(\tau)}{\sum_{m=1}^D \hat{r}_{1,m}(\tau)} = \frac{\hat{r}_{1,u}(\tau)}{\hat{r}_1(\tau)}. \quad (15)$$

In Fig. 2, we plot the $p_u(\tau)$ profile for the $(3, 6, 50)$ ensemble and $\epsilon = 0.45$. We consider two time instants: $\tau = 5$ (\square) and $\tau = 15$ (\circ), i.e., a time instant corresponding to the initial decoding phase and one corresponding to the steady state phase. As we discussed above, in the initial decoding phase we remove degree-one check nodes uniformly from all chain positions. In the case $\tau = 5$ (\square) the cumulative probability of removing a check node from positions 1 – 4 or 48 – 52 is less than 0.3. Since ϵ is larger than the BP threshold of the $(3, 6)$ code, i.e. $\epsilon_{(3,6)} = 0.4295$, no significant fraction degree-one check nodes is created in the center positions during the initial phase. At time $\tau^* \approx 10$ (see Fig.1(a)), all positions but those in the boundaries have run out of degree-one check nodes and the dynamics of the decoding process are described by a decoding wave which moves from the boundaries towards the middle [3]. For the case $\tau = 15$ in Fig. 2, the peaks of $p_u(\tau)$ roughly indicate where the decoding wave has its rapid rise.

D. A lower bound on τ^*

The time τ^* where the steady state phase begins is a function of the underlying ensemble (l, r) , the chain length L and the channel parameter ϵ . A lower bound on τ^* , that we denote by $\bar{\tau}$, can be obtained by ignoring the low-rate terminations at both sides of the (l, r, L) code graph and assuming a regular (l, r) -regular LDPC block code of length $n = ML$ operating above the (l, r) BP threshold. $\bar{\tau}$ is computed as the the expected time for which this ensemble runs out of degree-one check nodes. The expected graph evolution of the degree distribution for the (l, r) -regular LDPC block ensemble over peeling decoding is known in closed-form, see [9], [11]. For each ϵ value, the expected number of degree-one check nodes normalized by the codelength n at iteration ℓ is

$$r_1^u(y, \epsilon) = \epsilon \frac{l}{r} \left(1 - \frac{l}{r}\right) y^{l-1} \left(y - 1 + (1 - \epsilon y^{l-1})^{r-1}\right), \quad (16)$$

where

$$y = \left(1 - \frac{\ell}{\epsilon n}\right)^{1/l}. \quad (17)$$

For $\epsilon > \epsilon_{\text{BP}(l,r)}$, we use (16) and (17) to compute $\bar{\tau}$ by simply taking $n = ML$ and $\tau = \ell/M$. If \bar{y} is the highest solution for $r_1^u(y, \epsilon) = 0$, then

$$\tau^*(l, r, L) \geq \bar{\tau} = L\epsilon \left(1 - (\bar{y})^l\right) \quad (18)$$

The lower bound to τ^* becomes tighter in the limit $L \rightarrow \infty$, in which the cumulative probability of removing degree-one check nodes from the boundary positions tends to zero and the code essentially behaves during the first phase of the decoding like the corresponding underlying (l, r) -regular LDPC block code. In Table II we show $\bar{\tau}$ for the ensemble $(3, 6, 50)$ and the ϵ values corresponding to Fig.1. In all cases we observe $\bar{\tau}$ is smaller than the beginning of the steady state phase in Fig. 1(a).

IV. COVARIANCE EVOLUTION

As shown in [8], the PD covariance evolution for LDPC ensembles, i.e., the evolution along decoding of moments of the form $\text{CoVar}[\mathcal{G}_{j,u}(\tau), \mathcal{G}_{z,x}(\tau)]$ for any pair (u, x) of positions and any pair of degrees (j, z) , can be estimated by solving an augmented system of differential equations, referred to as covariance evolution. We define

$$f_{ju,zx}(\mathcal{G}(\tau)) = \frac{\mathbb{E} \left[\left(\mathcal{G}_{j,u}(\tau + \frac{1}{M}) - \mathcal{G}_{j,u}(\tau) \right) \left(\mathcal{G}_{z,x}(\tau + \frac{1}{M}) - \mathcal{G}_{z,x}(\tau) \right) \middle| \mathcal{G}(\tau) \right]}{1/M^2} \quad (19)$$

for $j, z \in \{1, \dots, r+1\}$ and $u, x \in \{1, \dots, D\}$. The system of differential equations in (10) is augmented with the set of equations in (20) (see next page). The solution for $\delta_{ju,zx}(\tau)$ is unique and, given the initial conditions

$$\hat{\mathcal{G}}_{j,u}(0) = \mathbb{E}[\mathcal{G}_{j,u}(0)], \quad (21)$$

$$\delta_{ju,zx}(0) = \mathbb{E}[\mathcal{G}_{j,u}(0)\mathcal{G}_{z,x}(0)] - \mathbb{E}[\mathcal{G}_{j,u}(0)]\mathbb{E}[\mathcal{G}_{z,x}(0)], \quad (22)$$

its deviation with respect the true covariance $\text{CoVar}[\mathcal{G}_{j,u}(\tau), \mathcal{G}_{z,x}(\tau)]$ is less than $M^{-1/2}$ [8]. Further, $\mathcal{G}(\tau)$ converges (in M) to a multivariate Gaussian distribution of dimension $D \times (r+1)$ with mean $\hat{\mathcal{G}}(\tau)$ and covariance matrix defined by $\delta_{ju,zx}(\tau)/M$ for $j, z \in \{1, \dots, r+1\}$ and $u, x \in \{1, \dots, D\}$. Therefore, any covariance moment vanishes in the limit $M \rightarrow \infty$ and $\mathcal{G}(\tau)$ concentrates around the mean $\hat{\mathcal{G}}(\tau)$ predicted by (10). The details of the computation of the correlations in (19) can be found in Appendix B. In Appendix C, we derive $\ell = 0$ covariances in (22) for the (l, r, L) ensemble. The derivatives of the function $f_{j,u}(\mathcal{G}(\tau))$ with respect to any component $\mathcal{G}_{q,m}(\tau)$, used in (20), are straightforward to compute given the closed-formed expression for $f_{j,u}(\mathcal{G}(\tau))$ derived Appendix A.

To estimate the (l, r, L) error probability we need to evaluate the variance of the process $r_1(\tau)$ in (12), whose mean evolution has been described in Section III-C. Given the solution to covariance evolution system of equations in (20), the variance of the process $r_1(\tau)$ is

$$\begin{aligned} \text{Var}[r_1(\tau)] &= \mathbb{E}[(r_1(\tau) - \hat{r}_1(\tau))^2] \\ &= \frac{1}{M} \sum_{u=1}^D \sum_{i=1}^D \delta_{1u,1i}(\tau) \doteq \frac{\delta_1(\tau)}{M}. \end{aligned} \quad (23)$$

In Fig. 3(a), we plot the solution for $\delta_1(\tau)$ computed numerically for the (l, r, L) ensemble with $L = 50$, $l = 3$, $r = 6$ and different ϵ values: 0.45 (\triangleleft), 0.46 (\circ), 0.47 (\triangleright). In (b), we normalize the curves by Δ_ϵ . The dashed line with the * marker, corresponds to $\delta_1(\tau)$ for a code with twice the length,

ϵ	L	$\bar{\tau}$
0.45	50	7.16
0.46	50	6.23
0.47	50	5.20
0.48	50	4.69
0.485	50	4.15
0.45	100	14.33

TABLE II
 $\bar{\tau}$ FOR THE $(3, 6, L)$ ENSEMBLE.

$$\frac{\partial \delta_{ju,zx}(\tau)}{\partial \tau} = \tag{20}$$

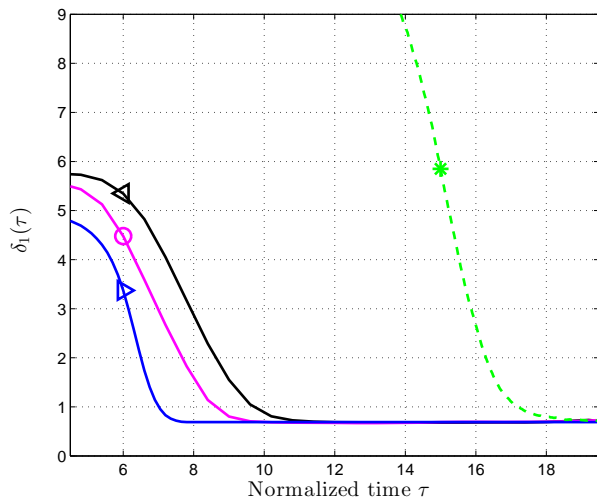
$$f_{j,u,zx}(\hat{\mathcal{G}}(\tau)) - f_{j,u}(\hat{\mathcal{G}}(\tau)) f_{z,x}(\hat{\mathcal{G}}(\tau)) + \sum_{q=1}^r \sum_{m=1}^D \delta_{ju,qm}(\tau) \frac{\partial f_{z,x}(\mathcal{G}(\tau))}{\partial \mathcal{G}_{q,m}(\tau)} \Big|_{\hat{\mathcal{G}}(\tau)} + \delta_{qm,xz}(\tau) \frac{\partial f_{j,u}(\mathcal{G}(\tau))}{\partial \mathcal{G}_{q,m}(\tau)} \Big|_{\hat{\mathcal{G}}(\tau)}$$

$$j, z \in \{1, \dots, r+1\}, u, x \in \{1, \dots, D\}.$$

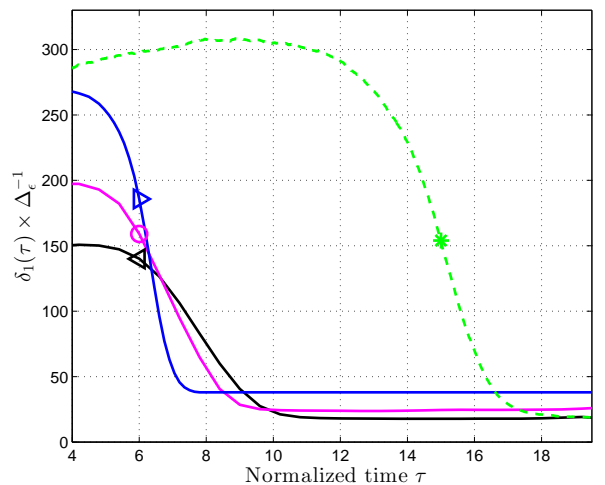
i.e., with $L = 100$ and $\epsilon = 0.45$. As $\hat{r}_1(\tau)$ in Fig.1, $\delta_1(\tau)$ shows an approximate a flat evolution in the steady state phase (as in the mean evolution case, small wiggles can be observed by magnification). Let $\delta_1(*)$ be $\delta_1(\tau)$ during this phase. Note also that, unlike the mean evolution during the steady state regime $\hat{r}_1(\tau)$ in (14), $\delta_1(*)$ does not show a strong dependence with ϵ for the range of values considered, i.e., an interval close to the ensemble's threshold. By dividing $\delta_1(*)$ by Δ_ϵ , see Fig. 3(b), results suggest that either $\delta_1(\tau)$ does not scale with Δ_ϵ or at least the scaling is sub-linear. We will simply assume that $\delta_1(*)$ is equal to a constant $\nu \in \mathbb{R}^+$ that depends on the underlying ensemble, i.e. $\nu = \nu(l, r)$. For the (3, 6) case, we observe $\nu \approx 0.69$. In Table III, we summarize the values of ν obtained for different ensembles. For a fixed coding rate, we observe that as the degrees of both variable and check nodes are increased, the variance parameter ν slightly increases as well.

l	r	ν
3	6	0.69
4	8	0.85
5	10	0.91
4	12	0.64
5	15	0.72
4	6	0.91

TABLE III
 ν PARAMETER FOR DIFFERENT (l, r, L) ENSEMBLES.



(a)



(b)

Fig. 3. In (a), we plot $\delta_1(\tau)$ computed for the (3, 6, $L = 50$) ensemble and $\epsilon = 0.45$ (\triangleleft), $\epsilon = 0.46$ (\circ) and $\epsilon = 0.47$ (\triangle). In (b), we normalize these curves by Δ_ϵ . In dashed line with * marker, we also include the solution to $\delta_1(\tau)$ for $L = 100$ and $\epsilon = 0.45$.

A. Process covariance at two time instants

We are interested in estimating the zero-crossing probability of the process $r_1(\tau)$, which corresponds to a decoding failure. Unlike for uncoupled ensembles, this error probability is not determined by the behavior of the decoder at a particular critical point in time, but errors happen more or less uniformly throughout the whole steady state phase. Recall that for the purpose of this paper we ignore errors which may happen in either the initial or the final phase since they are very rare.

A first naive estimate is to assume that, provided the Gaussian distribution of $r_1(\tau)$ at the steady state phase τ with known mean and variance, errors occur with the same probability at any time τ in this phase and that such probability is given as the probability of an univariate Gaussian with mean $\hat{r}_1(\tau^*)$ and variance $\delta_1(\tau^*)$ to take a negative value. Such an estimate ignores the correlations along time and would therefore be considerably off. Let us therefore discuss how we can incorporate these correlations. More precisely, in addition to the the mean and variance of $r_1(\tau)$ at a particular time τ , we need to estimate the process covariance along time, namely

$$\phi_1(\zeta, \tau) \doteq \mathbb{E}[r_1(\zeta)r_1(\tau)] - \hat{r}_1(\tau + \zeta)\hat{r}_1(\tau), \tag{24}$$

for some $\tau > \zeta$. The expectation is defined over the joint probability density function $p_{\mathcal{G}(\zeta), \mathcal{G}(\tau)}(g(\zeta), g(\tau))$. While this quantity can in principle be computed analytically by a procedure similar to covariance evolution, the dimension of the

associated system of differential equations makes prohibitive such approach. In fact, $\phi_1(\zeta, \tau)$ (or a quantity very related to it) has been analyzed already in the literature. More precisely, in [23] the authors prove that the covariance between BP messages at any iteration in a LDPC code graph decays exponentially fast with the distance in the graph between the related nodes. In terms of the peeling decoder formulation, this means that the correlation between the local residual DD of two subregions of the LDPC graph decays exponentially with the distance in the graph between such subregions. Recall that, during the steady state phase, the residual DD process $\mathcal{G}(\tau)$ has a strong spatial component since there are two decoding waves moving from the boundaries to the center [3] and each decoding time τ corresponds to a certain region of the graph where variable nodes are being revealed. Putting all together, we can conclude that, during the steady state phase, $\phi_1(\zeta, \tau)$ in (24) has to decay exponentially with $|\tau - \zeta|$:

$$\phi_1(\zeta, \tau) \approx \frac{\nu}{M} e^{-\theta|\tau - \zeta|}, \quad (25)$$

where θ , as shown later, is a parameter that depends on the (l, r) ensemble and the coupling pattern of the LDPC code. In this paper, we resort to a simple numerical procedure to compute decay parameter θ . First, we express the correlation in (24) in a more convenient way:

$$\begin{aligned} & \mathbb{E}[r_1(\zeta)r_1(\tau)] \\ &= \int \int r_1(\zeta)r_1(\tau) p_{\mathcal{G}(\zeta), \mathcal{G}(\tau)}(g(\zeta), g(\tau)) dg(\zeta)dg(\tau) \\ &= \int r_1(\zeta) \mathbb{E}[r_1(\tau)|g(\zeta)] p_{\mathcal{G}(\zeta)}(g(\zeta)) dg(\zeta), \end{aligned} \quad (26)$$

where the expectation inside the integral in (26) is taken with respect the conditional probability distribution

$$p_{\mathcal{G}(\tau)|g(\zeta)}(g(\tau)), \quad (27)$$

i.e. the graph DD probability density function at τ if the graph DD at ζ is $g(\zeta)$. Note that, for any DD $g(\zeta)$, we can easily evaluate $\mathbb{E}[r_1(\tau)|g(\zeta)]$ using the expected graph evolution results presented in Section III. Regarding the conditional distribution $p_{\mathcal{G}(\zeta)}(g(\zeta))$, for sufficiently large M it is well approximated by a multivariate Gaussian distribution, whose first and second order moments can be computed at any time ζ as shown in Sections III and IV. Unfortunately, the integral (26) lacks of close form. In this paper, we adopt a Monte Carlo approach to approximate $\phi_1(\zeta, \tau)$. For any pair (ζ, τ) , we draw N samples of $\mathcal{G}(\zeta)$. This task is straightforward since $\mathcal{G}(\zeta)$ Gaussian distributed. Let \mathcal{S} be the collection of the N graph DD samples. The integral in (26) is approximated by a sum of the form

$$\frac{1}{N} \sum_{g(\zeta) \in \mathcal{S}} r_1(\zeta) \mathbb{E}[r_1(\tau)|g(\zeta)]. \quad (28)$$

In the limit of $N \rightarrow \infty$, the sampled time covariance

$$\phi_1^N(\zeta, \tau) \doteq \frac{1}{N} \sum_{g(\zeta) \in \mathcal{S}} r_1(\zeta) \mathbb{E}[r_1(\tau)|g(\zeta)] - \hat{r}_1(\zeta) \hat{r}_1(\tau) \quad (29)$$

converges to the true covariance $\phi_1(\zeta, \tau)$ [24]. In Fig. 4, we plot $M\phi_1^N(\zeta, \tau)$ for the $(3, 6, L = 50)$ ensemble, $\epsilon = 0.45$

and $N = 200$. We have fixed ζ to 13 (\triangleleft) and 16 (\diamond) and evaluate $\phi_1^N(\zeta, \tau)$ for different τ values. In thin solid line, we have also included an estimation to $M\phi_1(\zeta, \tau)$ for $\zeta = 13$ computed by simulating 500 decoding trajectories with a code $M = 1000$ bits per position. As predicted, the covariance decay exponentially with $|\tau - \zeta|$. It is important to remark that $\phi_1^N(\zeta, \tau)$ is a quantity obtained using exclusively the equations that predict the (l, r, L) ensemble mean and variance graph evolution derived in Sections III and IV respectively. In Table IV, we show the θ value computed for different (l, r, L) ensembles. As we can observe, for fixed rate, the covariance decays slightly faster as we increase check degree.

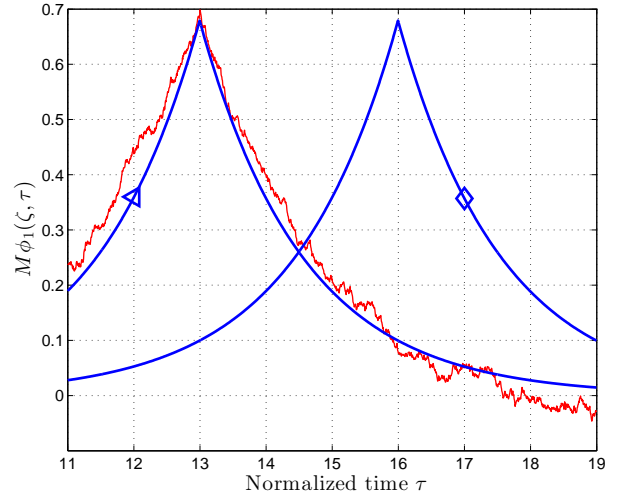


Fig. 4. Monte Carlo estimate $\phi_1^N(\zeta, \tau)$ to the $r_1(\tau)$ process covariance for the $(3, 6, L = 50)$ ensemble and $N = 200$ samples. We have fixed ζ to 13 (\triangleleft) and 16 (\diamond) and evaluated $\phi_1^N(\zeta, \tau)$ for different τ values. For $\zeta = 13$, we have also included an estimation to $\phi_1(\zeta, \tau)$ computed using 500 simulated decoding trajectories for the $(3, 6, 50)$ ensemble with $M = 1000$ bits per position.

l	r	θ
3	6	0.59
4	8	0.61
5	10	0.63
4	12	0.84
5	15	0.88
4	6	0.51

TABLE IV
 θ PARAMETER FOR DIFFERENT (l, r, L) ENSEMBLES.

The correlation decay of the process $r_1(\tau)$, and hence the θ parameter in (25), not only depends on the regular (l, r) ensemble that we use to construct the LDPC convolutional ensemble, but also on coupling pattern utilized to generate it. To illustrate this dependence, consider an expanded (l, r, L) ensemble, denoted by $\mathcal{E}(l, r, L, w)$ where w is a positive integer. In the $\mathcal{E}(l, r, L, w)$ ensemble, the l edges of a variable node at position u are respectively connected to positions $u, u + w, u + 2w, \dots, u + w(l - 1)$ if u is odd and to positions $u, u + 1, u + 2, \dots, u + (l - 1)$ if u is even. We illustrate the $(3, 6, L, 2)$ ensemble in Fig. 5. As we expand the coupling

pattern by increasing w , we expect an slower decay of the covariance of the process $r_1(\tau)$ along the time and, thus, smaller θ values. In Fig. 6, we plot $M\phi_1^N(\zeta, \tau)$ with $N = 200$ computed for the standard $(3, 6, 100)$ ensemble (\triangleleft) and the $\mathcal{E}(3, 6, 100, w)$ ensemble with $w = 2$ (\triangleright) and $w = 4$ (\square). ζ is fixed to 29. For each case, in thin dashed lines we also include an estimate to $M\phi_1(\zeta, \tau)$ computed using 500 simulated $r_1(\tau)$ trajectories for $M = 1000$ bits per positions. We have normalized the curves by the steady state variances ν , placing the peak of all curves to 1. As expected, the covariance between $r_1(\tau)$ and $r_1(\zeta = 29)$ is higher for larger w values, where the estimated θ values are, respectively, $\theta = 0.59$, $\theta = 0.28$ ($w = 2$) and $\theta = 0.17$ ($w = 4$).

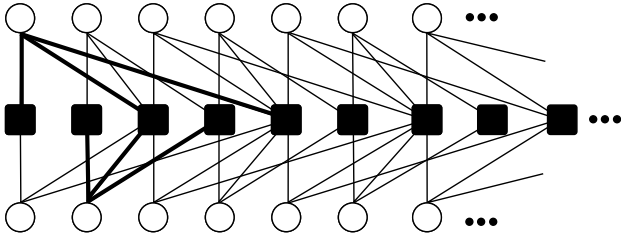


Fig. 5. A graphical representation of the $(3, 6, L, w)$ ensemble for $w = 2$. In thick lines, we illustrate the connections of a variable node placed at an odd position and a variable node at an even position.

At this point, we have all the ingredients we need to predict the survival probability of the process $r_1(\tau)$. Before concluding the present section, we finally want to emphasize that the triple (γ, ν, θ) only depends on the underlying ensemble (l, r) and the coupling pattern. The larger we choose L , the longer the process $r_1(\tau)$ remains in the steady state phase and thus the larger the error probability will be. However, the intrinsic properties of the $r_1(\tau)$ process do not vary if we increase the chain length L . To illustrate this property, in Fig. 1 and Fig. 3

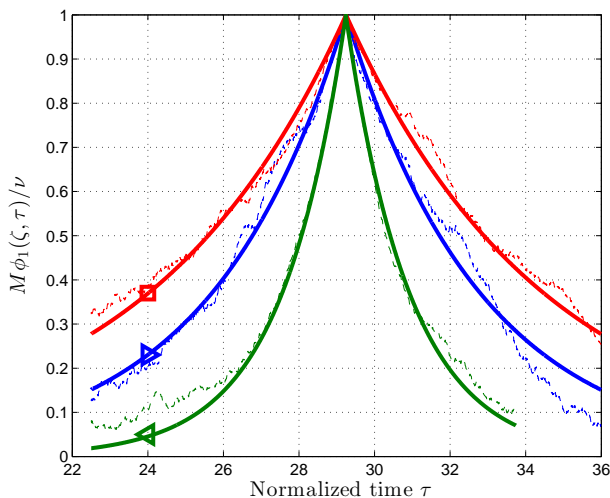


Fig. 6. Estimate to the $r_1(\tau)$ time-covariance $\phi_1^N(\zeta, \tau)$ with $N = 200$ samples for the standard $(3, 6, 100)$ ensemble (\triangleleft) and the $\mathcal{E}(3, 6, 100, w)$ ensemble with $w = 2$ (\triangleright) and $w = 4$ (\square). We have fixed ζ to 29. In thin dashed lines we also include an estimate to $M\phi_1(\zeta, \tau)$ computed using 500 simulated $r_1(\tau)$ trajectories.

we have included results for both the $(l = 3, r = 6, L = 50)$ ensemble and the $(l = 3, r = 6, L = 100)$ ensemble, i.e. two ensembles constructed from the same regular code but with different chain lengths.

V. ERROR PROBABILITY PREDICTION USING ORNSTEIN-UHLENBECK PROCESSES

In the previous sections, we have provided a statistical characterization of the process $r_1(\tau)$ for the (l, r, L) ensemble when used for transmission over the BEC and decoded via PD. As proved in [8], $r_1(\tau)$ is a Markov process that converges (in the number M of bits per position of the code) to a Gaussian process. Covariance evolution for the (l, r, L) ensemble shows that $r_1(\tau)$ in the steady state phase is essentially a constant mean and constant variance process whose temporal covariance only depends on the time difference between the two time instants considered. In other words, in the steady state phase, $r_1(\tau)$ is well modeled by a stationary Gaussian Markov process. In the light of these results, the evaluation of the (l, r, L) decoding error probability is intimately linked with the first-passage time statistics of stationary Gaussian Markov processes. Indeed, a stationary Gaussian Markov process $X(t)$ can only be one of the two following types [12], [25]:

- If $t_1 < t_2 < \dots < t_n$, $X(t_1), \dots, X(t_n)$ are mutually-independent Gaussian random variables.
- There exists a constant α such that if $t_1 < t_2 < \dots < t_n$, then $X(t_1), \dots, X(t_n)$ are jointly distributed by a multivariate Gaussian with common mean and variance and covariance function $\text{CoVar}[X(t+T), X(t)] \propto \exp^{-\alpha T}$,

where the latter type of Gaussian Markov process is called a Ornstein-Uhlenbeck (OU) process. Based on the first and second moments of $r_1(\tau)$, the OU process emerges as the only compatible model to predict the survival probability of the decoding process $r_1(\tau)$. In the following we describe the properties and parameters of OU processes and link them with those already computed for $r_1(\tau)$, namely γ , ν and θ computed in Sections III-B, IV and IV-A respectively.

A. Ornstein-Uhlenbeck Processes

A OU process is a stationary Gaussian Markov process evolving via the following stochastic equation [12]:

$$X(t) = X_0 e^{-at} + \sqrt{2b} e^{-at} \int_0^t \omega(u) e^{au} du, \quad (30)$$

where $\omega(t)$ is a white noise with zero mean and unit variance, a is a real constant and X_0 is the initial condition. Consider samples uniformly taken from $X(t)$ every Ω seconds, being X_i the i -th sample. The mean of X_i is given by

$$\mathbb{E}[X_i] = X_0 e^{-ai\Omega} = X_0 g^i, \quad g \doteq e^{-a\Omega} \quad (31)$$

Similarly, the covariance function is given by

$$\mathbb{E}[(X_i - \mathbb{E}[X_i])(X_j - \mathbb{E}[X_j])] = \frac{b}{a} (g^{|i-j|} - g^{i+j}). \quad (32)$$

Therefore, for sufficiently large $i + j$,

$$X_i \sim \mathcal{N}(x|0, \frac{b}{a}), \quad (33)$$

$$\mathbb{E}[(X_i - \mathbb{E}[X_i])(X_j - \mathbb{E}[X_j])] = \frac{b}{a} (g^{|i-j|}). \quad (34)$$

The OU process presents constant mean and variance and an exponentially covariance decay and, thus, it constitutes a consistent model to the evolution of $r_1(\tau)$ in the steady state phase of the PD process. By using $\mathbb{E}[r_1(\tau)] \approx \gamma(l, r)\Delta_\epsilon$, $\text{Var}(r_1(\tau)) \approx \nu(l, r)M^{-1}$ and that $\text{CoVar}[r_1(\tau), r_1(\zeta)] \approx \nu M^{-1} \exp(\theta(l, r)|\tau - \zeta|)$, the process $r_1(\tau) - \hat{r}_1(*)$ can be identified to as an OU process with parameters:

$$a = \theta, \quad b = \frac{\theta\nu}{M}, \quad (35)$$

where we have taken $\Omega = M^{-1}$, i.e., the normalized time for a single PD iteration.

B. First passage time distribution

The distribution of the first passage time (FPT) of an Ornstein-Uhlenbeck process to a fixed boundary s is of interest in a variety of fields. Unlike the density of the first passage time to a fixed boundary for Brownian motion, the FPT density for the OU process is not known in closed form. However, explicit expressions are known for the moments of the first passage time. We refer the reader to [18], [26], [17], [27], [19], [28] as a non-rigorous sample of works in the field. Define FPT as

$$T_s = \inf_{t \geq 0} \{t : X_t \geq s\}. \quad (36)$$

As $\frac{s}{b/a} \rightarrow 0$, evaluating the pdf of T_s becomes a hard problem and we lack of closed form expressions [27]. In our context, s is given by $\hat{r}_1(*) = \gamma\Delta_\epsilon$ and

$$\frac{s}{b/a} = \frac{\gamma\Delta_\epsilon M}{\nu}. \quad (37)$$

Hence, $\frac{s}{b/a} \rightarrow 0$ represents the case in which either M is too small or we are too close to the BP threshold. In both cases we know the error probability is close to one. In [17], the authors show that the first-passage time p.d.f. $p(T_s)$ converges with growing $\frac{s}{b/a}$ to an exponential distribution

$$p(T_s) \sim \frac{1}{\mu_0} e^{-t/\mu_0}, \quad (38)$$

where μ_0 is the OU mean first-passage time from the zero initial state to the boundary s . An explicit expression is known for μ_0 [18], [17]:

$$\mu_0 = \frac{\sqrt{2\pi}}{a} \int_0^{\frac{s}{\sqrt{b/a}}} \Phi(z) e^{\frac{1}{2}z^2} dz, \quad (39)$$

where $\Phi(z)$ is the cdf of a Gaussian distribution with zero mean and unit variance. In our decoding scenario, μ_0 represents the average survival time once $r_1(\tau)$ has entered the steady state phase. In terms of the parameters of $r_1(\tau)$ in (35), μ_0 is given by:

$$\mu_0(l, r, M, \epsilon) = \frac{\sqrt{2\pi}}{\theta} \int_0^{\alpha\sqrt{M}\Delta_\epsilon} \Phi(z) e^{\frac{1}{2}z^2} dz, \quad (40)$$

where $\alpha \doteq \gamma\nu^{-1/2}$. Note that the integral in (40) diverges; the expected failure time grows exponentially fast with M and Δ_ϵ . Note also that $\mu_0 \propto \theta^{-1}$, which means that the coupling pattern can be further optimized to improve the finite-length performance of SC-LDPC codes. As we show in Fig. 6, we can make θ arbitrarily small by expanding the coupling pattern. However, note that the effect in μ_0 of a variation in θ is mild compared to the improvement we can achieve by slightly increasing the number M of bits per position, since μ_0 grows exponentially fast with M but linearly with θ^{-1} .

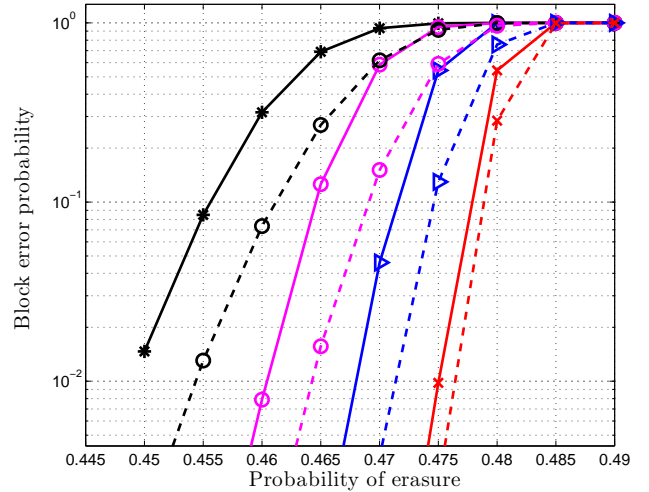


Fig. 7. Simulation error probability curves (solid lines) along with the prediction using the expression in (41) (dashed lines) for the ensemble $(3, 6, 50, M)$ and $M = 500$ (*), $M = 1000$ (o), $M = 2000$ (\triangleright) and $M = 4000$ (\times).

C. Scaling law for the (l, r, L) ensemble

The first passage-time probability distribution in (38) along with (40) constitutes the necessary tools to estimate the decoding error probability. The steady state phase roughly lasts between $\tau^* = \tau^*(l, r, L, \epsilon)$, which as explained in Section III-D can be lower bound by $\bar{\tau} = \bar{\tau}(l, r, L, \epsilon)$, and ϵL . Therefore, the block error probability of the ensemble can be estimated using the exponential distribution c.d.f., yielding the following scaling law (SL)

$$\begin{aligned} \mathbb{E}[P_B(l, r, L, M, \epsilon)] &\approx 1 - \exp\left(-\frac{\epsilon L - \tau^*}{\mu_0}\right) \\ &\leq 1 - \exp\left(-\frac{\epsilon L - \bar{\tau}}{\mu_0}\right) \\ &= 1 - \exp\left(-\frac{\epsilon L \bar{y}^l}{\mu_0}\right) \end{aligned} \quad (41)$$

where \bar{y}^l is the solution to the equation $r_1^u(y, \epsilon) = 0$ in (16). In Fig. 7 we compare simulated block error probability curves (solid lines) along with the prediction using the expression in (41) (dashed lines). The number M of bits per position is: $M = 500$ (*), $M = 1000$ (o), $M = 2000$ (\triangleright) and $M = 4000$ (\times). Up to a shift that vanishes with growing M , the SL captures the scaling between block error rate, chain

length L , bits per positions M and the gap to the threshold Δ_ϵ . Similar results and conclusions hold when we consider other (l, r, L) ensembles. For instance, in Fig. 8, for $M = 4000$, we include both simulation performance curves and the SL for the ensembles $(4, 8, L = 50)$ (\circ), $(5, 10, L = 50)$ (\triangleright), $(3, 6, L = 100)$ ($+$) and $(3, 6, L = 50)$ (\times). As shown, for sufficiently large M , our model is flexible enough to provide an accurate estimate for different ensembles and chain lengths.

Although our scaling law captures the main dependence on the various parameters it can still be improved. In particular, one can see that there is a systematic “shift” between the actual curves and the curves predicted via our scaling law. Where does this shift come from?

As discussed in Section V-B, the SL in (41) is based on an asymptotic result for the FPT pdf of OU processes that holds in the limit $\Delta_\epsilon M \rightarrow \infty$. To derive a better approximation to the performance of the (l, r, L) ensemble for low and moderate M values one would need to take into consideration corrections on the FPT pdf for the OU process when the boundary is close to zero. To the best of our knowledge, there do not exist closed-form expressions for the FPT pdf in this regime. In addition, there are some other effects which we have not taken into account. In particular, our model only captures the decoding failures once the decoder is in its “steady” state but it ignores the effects at the boundary. It is an interesting and challenging problem to take these effects into account.

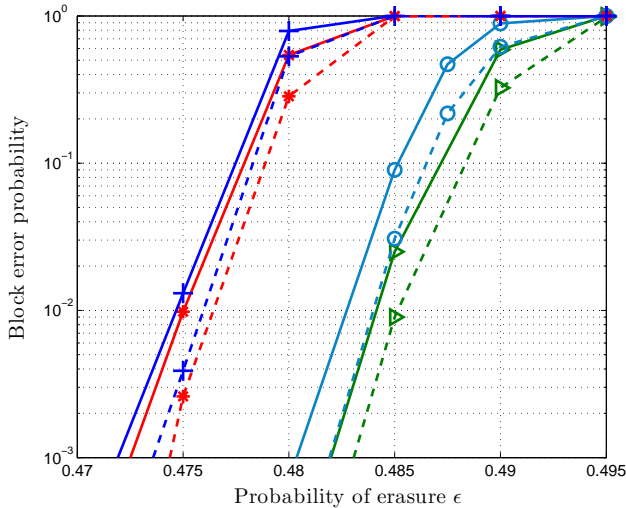


Fig. 8. Simulation error probability curves (solid lines) along with the prediction using the expression in (41) (dashed lines) for the ensembles $(4, 8, L = 50)$ (\circ), $(5, 10, L = 50)$ (\triangleright), $(3, 6, L = 100)$ ($+$) and the $(3, 6, L = 50)$ (\times) and $M = 4000$.

The proposed model to estimate the finite-length performance of convolutional LDPC ensembles provides intuitive understanding of the dynamics of the decoding process and the main scaling rules between code parameters and the final error rate. Through the covariance decay parameter θ , we have a notion of how the effect of the coupling pattern may affect to the ensemble finite-length performance. An optimization of the coupling pattern to boost performance is therefore an interesting open question. Comparison with

simulated performance results shows that the prediction becomes accurate for reasonably values of the number M of bits per position, around thousand of bits. This scenario is well suited for practical applications where convolutional LDPC ensembles are excellent candidates for future communication standards such as optical communications [29] and wireless digital broadcasting [30].

D. Threshold saturation and limiting scaling function

In [7], the performance of LDPC codes was tested for a wide range of scaling functions $L = f(M)$. It was observed that the threshold saturation effect, i.e. a vanishing error probability in the limit $M \rightarrow \infty$ for $\epsilon \leq \epsilon_{\text{MAP}}(l, r)$, happens even though if L grows much faster than M . In particular, we conjectured that the threshold saturation effect is lost only when the chain length L grows at least exponentially fast with M . The scaling law for LDPC ensembles in (41) is consistent with such conjecture. By (41), as long as the following limit diverges

$$\lim_{M \rightarrow \infty} \frac{\mu_0(l, r, M, \epsilon)}{L} \rightarrow \infty, \quad (42)$$

then the ensemble presents a BP threshold arbitrarily close to $\epsilon_{\text{MAP}}(l, r)$, and thus very close to channel capacity. For sufficiently large M , we have

$$\begin{aligned} \mu_0(l, r, M, \epsilon) &= \frac{\sqrt{2\pi}}{\theta} \int_0^{\alpha\sqrt{M}\Delta_\epsilon} \Phi(z) e^{\frac{1}{2}z^2} dz \\ &\approx \frac{\sqrt{2\pi}}{\theta} \int_0^{\alpha\sqrt{M}\Delta_\epsilon} e^{\frac{1}{2}z^2} dz \\ &= \sum_{n=0}^{\infty} \frac{2^{-n}}{n!(2n+1)} (\alpha\Delta_\epsilon)^{2n+1} M^{\frac{2n+1}{2}}, \end{aligned} \quad (43)$$

where the equality is obtained by using the series expansion $\exp(x) = \sum_n x^n/n!$. The dominant term in the sum in (44) is M^n . Clearly, (42) diverges for any scaling of the form $f(M) = aM^b$, where a and b are real constants. However, if $f(M) = a \exp(bM)$ then there exists two real constants (a, b) for which the following limit is zero

$$\lim_{M \rightarrow \infty} \frac{\mu_0(l, r, M, \epsilon)}{f(M)} = \frac{\sum_{n=0}^{\infty} \frac{2^{-n}}{n!(2n+1)} (\alpha\Delta_\epsilon)^{2n+1} M^{\frac{2n+1}{2}}}{a \sum_{n=0}^{\infty} b^n \frac{M^n}{n!}}, \quad (45)$$

which can be easily proved by comparing both sums component wise. This coincides with our conclusions in [7].

VI. CONCLUSIONS AND FUTURE WORK

In this work we have analyzed the decoding of finite-length convolutional LDPC codes over the BEC using the peeling decoder. By extending the methodology applied in [8] to study finite-length LDPC ensembles, we have determined and solved covariance evolution, i.e., the system of differential equations that encodes the dynamics of the decoding process. We have shown that the statistical evolution of the normalized number

of degree-one check nodes along the peeling decoding process, i.e. the $r_1(\tau)$ process, is of a completely different nature with respect to the case of standard (l, r, ν) -regular LDPC block codes. For sufficiently large chain lengths L , decoding failures can happen more or less uniformly throughout the whole decoding process. The statistics of the graph evolution process, that we compute has the solution to covariance evolution, fit those of an appropriately chosen Ornstein-Uhlenbeck process, which is used to propose a scaling law to predict the LDPC code finite-length performance based on known expressions for the first time-passage distribution of an OU process. The scaling law contains four parameters: the ensemble threshold, mean parameter γ , covariance parameter ν and spatial covariance θ . The threshold can be determined through standard DE techniques and the triple (γ, ν, θ) for each ensemble (l, r, L) is computed directly given the solution to covariance evolution.

The closed-form SL proposed in this paper provides code designers practical understanding on the main scaling between error rate and the different code parameters. On the other hand, the real value of scaling law will emerge if all quantities can be computed efficiently, and if this can be used as the basis for code optimization as this was done for uncoupled LDPC ensembles. A close form expression to evaluate the triple (γ, ν, θ) is one of our future lines of research. Another important aspect is analyzing the effect over the SL proposed of a window decoder [6]. Besides, an extension to advanced coupling structures such as randomized connections between sections [3], coupled codes generated by connecting two LDPC codes forming a loop [31] and protograph-based constructions [2], [22] will be of undoubtedly practical interest.

REFERENCES

- [1] S. Kudekar, T. Richardson, and R. Urbanke, "Spatially Coupled Ensembles Universally Achieve Capacity under Belief Propagation," *IEEE Transactions on Information Theory*, vol. 59, no. 12, pp. 7761 – 7813, Dec. 2013.
- [2] M. Lentmaier, A. Sridharan, D. J. Costello, Jr, and K. Zigangirov, "Iterative decoding threshold analysis for LDPC convolutional codes," *IEEE Transactions on Information Theory*, vol. 56, no. 10, pp. 5274 –5289, Oct. 2010.
- [3] S. Kudekar, T. Richardson, and R. Urbanke, "Threshold saturation via spatial coupling: Why convolutional LDPC ensembles perform so well over the BEC," *IEEE Transactions on Information Theory*, vol. 57, no. 2, pp. 803–834, Feb. 2011.
- [4] A. Jimenez Felstrom and K. Zigangirov, "Time-varying periodic convolutional codes with low-density parity-check matrix," *IEEE Transactions on Information Theory*, vol. 45, no. 6, pp. 2181 –2191, Sept. 1999.
- [5] A. Pusane, A. Feltstrom, A. Sridharan, M. Lentmaier, K. Zigangirov, and D. J. Costello, Jr, "Implementation aspects of LDPC convolutional codes," *IEEE Transactions on Communications*, vol. 56, no. 7, pp. 1060 –1069, July 2008.
- [6] A. Iyengar, M. Papaleo, P. Siegel, J. Wolf, A. Vanelli-Coralli, and G. Corazza, "Windowed decoding of protograph-based LDPC convolutional codes over erasure channels," *IEEE Transactions on Information Theory*, vol. 58, no. 4, pp. 2303 – 2320, April 2011.
- [7] P. M. Olmos and R. Urbanke, "Scaling behavior of Convolutional LDPC ensembles over the BEC," in *Proc. IEEE International Symposium on Information Theory (ISIT)*, St. Petersburg, Russia, Aug. 2011, pp. 1816 –1820.
- [8] A. Amraoui, A. Montanari, T. Richardson, and R. Urbanke, "Finite-length scaling for iteratively decoded LDPC ensembles," *IEEE Transactions on Information Theory*, vol. 55, no. 2, pp. 473 –498, Feb. 2009.
- [9] M. Luby, M. Mitzenmacher, M. Shokrollahi, and D. Spielman, "Efficient erasure correcting codes," *IEEE Transactions on Information Theory*, vol. 47, no. 2, pp. 569 –584, Feb. 2001.
- [10] A. Amraoui, R. Urbanke, and A. Montanari, "Finite-length scaling of irregular LDPC code ensembles," in *Proc. IEEE Information Theory Workshop (ITW)*, Rotorua, New Zealand, Aug. 2005.
- [11] T. J. Richardson and R. Urbanke, *Modern Coding Theory*. Cambridge University Press, Mar. 2008.
- [12] I. Karatzas and S. E. Shreve, *Brownian Motion and Stochastic Calculus (Graduate Texts in Mathematics)*, 2nd ed. Springer, Aug. 1991.
- [13] J. M. Beaulieu, D.-C. Jhwueng, C. Boettiger, and B. C. O'Meara, "Modeling Stabilizing Selection: Expanding the Ornstein-Uhlenbeck model of Adaptive Evolution," *Evolution*, vol. 66, no. 8, pp. 2369–2383, August 2012.
- [14] O. Aalen and H. K. Gjessing, "Survival models based on the Ornstein-Uhlenbeck Process," *Lifetime Data Analysis*, vol. 10, no. 4, pp. 407–423, 2004.
- [15] P. Collin-Dufresne and R. S. Goldstein, "Do Credit Spreads Reflect Stationary Leverage Ratios?" *The Journal of Finance*, vol. 56, no. 5, pp. pp. 1929–1957, 2001.
- [16] O. Onalan, "The Ornstein-Uhlenbeck Processes driven by Lévy process and Application to Finance," in *Electronic Engineering and Computing Technology*, ser. Lecture Notes in Electrical Engineering. Springer Netherlands, 2010, vol. 60, pp. 443–453.
- [17] A. G. Nobile, L. M. Ricciardi, and L. Sacerdote, "Exponential trends of Ornstein-Uhlenbeck First-Passage-time densities," *Journal of Applied Probability*, vol. 22, no. 2, pp. 360–369, 1985.
- [18] M. U. Thomas, "Some Mean First-Passage Time Approximations for the Ornstein-Uhlenbeck process," *Journal of Applied Probability*, vol. 12, no. 3, pp. 600–604, 1975.
- [19] G. Ehrhardt, S. Majumdar, and A. Bray, "Persistence exponents and the statistics of crossings and occupation times for gaussian stationary processes," *Phys Rev E Stat Nonlin Soft Matter Phys*, vol. 69, no. 1, 2004.
- [20] M. Lentmaier, D. Mitchell, G. Fettweis, and D. J. Costello, Jr, "Asymptotically regular LDPC codes with linear distance growth and thresholds close to capacity," in *Proc. Information Theory and Applications (ITA) Workshop*, San Diego, CA, Feb. 2010.
- [21] D. Mitchell, A. Pusane, M. Lentmaier, and D. J. Costello, Jr, "Exact free distance and trapping set growth rates for LDPC convolutional codes," in *Proc. IEEE International Symposium on Information Theory (ISIT)*, St. Petersburg, Russia, Aug. 2011, pp. 1096 –1100.
- [22] M. Stinner and P. M. Olmos, "Analyzing Finite-length Protograph-based Spatially Coupled LDPC Codes," in *ArXiv e-prints. Accepted for presentation at IEEE 2014 International Symposium on Information Theory (ISIT)*, Honolulu, USA, 2014. [Online]. Available: <http://arxiv.org/abs/1401.8090>
- [23] S. Kudekar and N. Macris, "Decay of Correlations for Sparse Graph Error Correcting Codes," *SIAM Journal on Discrete Mathematics*, vol. 25, no. 2, pp. 956–988, 2011.
- [24] K. P. Murphy, *Machine learning: a probabilistic perspective*. MIT press, 2012.
- [25] J. L. Doob, *The Brownian Movement and Stochastic Equations*, ser. Second Series. Annals of Mathematics, 1942, vol. 43, no. 2.
- [26] L. M. Ricciardi and S. Sato, "First-passage-time density and moments of the ornstein-uhlenbeck process," *Journal of Applied Probability*, vol. 25, no. 1, pp. 43–57, 1988.
- [27] D. T. Gillespie, "Exact numerical simulation of the Ornstein-Uhlenbeck process and its integral," *Physical review. E, Statistical physics, plasmas, fluids, and related interdisciplinary topics*, vol. 54, no. 2, pp. 2084–2091, 1996.
- [28] P. J. Thomas, "A lower bound for the first passage time density of the suprathreshold ornstein-uhlenbeck process," *Journal of Applied Probability*, vol. 48, no. 2, pp. 420–434, 06 2011. [Online]. Available: <http://dx.doi.org/10.1239/jap/1308662636>
- [29] F. Chang, K. Onohara, and T. Mizuochi, "Forward error correction for 100 G transport networks," *Communications Magazine, IEEE*, vol. 48, no. 3, 2010.
- [30] "Digital Video Broadcasting-t2 standard, EN 302 755 v.1.3.1." [Online]. Available: <http://www.dvb.org/technology/dvbt2/index.xml>
- [31] D. Truhachev, D. Mitchell, M. Lentmaier, and D. J. Costello, Jr, "Improving spatially coupled LDPC codes by connecting chains," in *Proc. IEEE International Symposium on Information Theory, Boston, United States*, 2012, pp. 468–472.

APPENDIX A

EXPECTED EVOLUTION IN ONE ITERATION OF THE PD

Here we show how to compute the expected evolution of the (l, r, L) graph DD in one PD iteration, namely

$$\mathbb{E}[R_{j,u}(\ell+1) - R_{j,u}(\ell)|\mathcal{G}(\ell)], \quad (46)$$

$$\mathbb{E}[V_u(\ell+1) - V_u(\ell)|\mathcal{G}(\ell)], \quad (47)$$

for $u \in \{1, \dots, D\}$ and $j = 1, \dots, r$. To keep the notation uncluttered, we omit the conditionality on $\mathcal{G}(\ell)$ and we denote

$$\Delta R_{j,u}(\ell) = R_{j,u}(\ell+1) - R_{j,u}(\ell), \quad (48)$$

$$\Delta V_u(\ell) = V_u(\ell+1) - V_u(\ell). \quad (49)$$

Let $\text{pos}(\ell)$ be the position at which we remove a degree-one check node at iteration ℓ . The actual check node that is removed is chosen uniformly at random from all degree-one check nodes at this position. The resulting probability distribution $P(\text{pos}(\ell) = u)$ is described by p_u in (15). Assume that $\text{pos}(\ell) = m$. It follows that the variable connected to this degree-one check node is placed at position u with probability

$$\lambda_{m,u}(\ell) = \frac{V_u(\ell)}{\sum_{i=m-(l-1)}^m V_i(\ell)} \quad (50)$$

if $u \in \{m - (l - 1), \dots, m\}$ and it is zero otherwise. When a check node from position m is removed, a check node at position u loses one edge with probability

$$\xi_{m,u}(\ell) = \sum_{i=u-(l-1)}^u \lambda_{m,i}(\ell). \quad (51)$$

Note that $\xi_{m,m}(\ell) = 1 \forall m$. The expected DD evolution at position $m = \text{pos}(\ell)$ is straightforward to compute since we just remove an edge connected to a check of degree one. Thus, $\mathbb{E}[R_{j,m}(\ell+1) - R_{j,m}(\ell)|\text{pos}(\ell) = m]$ is equal to -1 for $j = 1$ and zero otherwise. Given $m = \text{pos}(\ell)$, the graph at position $u \neq m$ loses one edge with probability $\xi_{m,u}(\ell)$. The edge removed is connected to a check node of degree j with probability

$$\frac{R_{j,u}(\ell)}{\sum_{q=1}^r R_{q,u}(\ell)}, \quad (52)$$

and, if this happens, the graph at u loses j edges of right degree j and wins $j - 1$ edges of right degree $j - 1$. Hence, the expected graph evolution at position u is

$$\mathbb{E}[\Delta R_{j,u}(\ell)|\text{pos}(\ell) = m] = j\xi_{m,u}(\ell) \frac{R_{j+1,u}(\ell) - R_{j,u}(\ell)}{\sum_{q=1}^r R_{q,u}(\ell)}, \quad (53)$$

where for $j = r$, $R_{j+1,u}(\ell) = 0$. Besides, again for $\text{pos}(\ell) = m$, we lose a variable at position u with probability $\lambda_{m,u}(\ell)$. Therefore,

$$\mathbb{E}[\Delta V_u(\ell)|\text{pos}(\ell) = m] = -\lambda_{m,u}(\ell). \quad (54)$$

Finally, the expected graph evolution after one iteration of the PD can be computed as follows. For $2 \leq j \leq (r - 1)$ we

get,

$$\begin{aligned} \mathbb{E}[\Delta R_{j,u}(\ell)] & \quad (55) \\ &= j \sum_{\substack{m=1 \\ m \neq u}}^D \xi_{m,u}(\ell) \frac{R_{j+1,u}(\ell) - R_{j,u}(\ell)}{\sum_{q=1}^r R_{q,u}(\ell)} p_m(\ell) \\ &= j \left(\frac{R_{j+1,u}(\ell) - R_{j,u}(\ell)}{\sum_{q=1}^r R_{q,u}(\ell)} \right) (\mathbf{p}^T \boldsymbol{\xi}_u - p_u(\ell)), \end{aligned}$$

where $\mathbf{p} \doteq [p_1(\ell) \dots p_D(\ell)]$ and $\boldsymbol{\xi}_u = [\xi_{1,u}, \xi_{2,u}, \dots, \xi_{D,u}]$. For the case $j = 1$, we just have to include degree-one check lost if position u is selected. Thus,

$$\begin{aligned} \mathbb{E}[\Delta R_{1,u}(\ell)] & \quad (56) \\ &= -p_u(\ell) + \left(\frac{R_{2,u}(\ell) - R_{1,u}(\ell)}{\sum_{q=1}^r R_{q,u}(\ell)} \right) (\mathbf{p}^T \boldsymbol{\xi}_u - p_u(\ell)). \end{aligned}$$

On the variable side we obtain

$$\mathbb{E}[\Delta V_u(\ell)] = - \sum_{m=1}^D \lambda_{m,u}(\ell) p_m(\ell). \quad (57)$$

APPENDIX B

COVARIANCE EVOLUTION IN ONE ITERATION OF THE PD

We are now interested in computing the second order moments for the (l, r, L) ensemble DD transition at one PD iteration:

$$\mathbb{E}[\Delta R_{j,u}(\ell) \Delta R_{z,x}(\ell)|\mathcal{G}(\ell)], \quad (58)$$

$$\mathbb{E}[\Delta V_u(\ell) \Delta V_x(\ell)|\mathcal{G}(\ell)], \quad (59)$$

$$\mathbb{E}[\Delta R_{j,u}(\ell) \Delta V_x(\ell)|\mathcal{G}(\ell)], \quad (60)$$

for $u, x \in \{1, \dots, D\}$ and $j, z \in \{1, \dots, r\}$. Note that we do not compute second order moments taken across different time instants. As in Appendix A, we omit the conditionality to $\mathcal{G}(\ell)$ and, to compute the expectations in (58)-(60), we average over all possible positions where a degree-one check node can be removed. For instance,

$$\begin{aligned} \mathbb{E}[\Delta R_{j,u}(\ell) \Delta R_{z,x}(\ell)] & \quad (61) \\ &= \sum_{m=1}^D \mathbb{E}[\Delta R_{j,u}(\ell) \Delta R_{z,x}(\ell)|\text{pos}(\ell) = m] p_m(\ell). \end{aligned}$$

We consider two different scenarios: $u \neq x$ and $u = x$. Namely, second order moments across different positions and within the same position.

1) *Different positions. Case $u \neq x$:* Assume that $x = u + c$, where c is a strictly positive integer. If $c \geq l$, then the DD at positions u and x cannot be modified at the same time because check nodes at two positions further away $l - 1$ positions do not share any variable node. Thus

$$\mathbb{E}[\Delta R_{j,u}(\ell) \Delta R_{z,x}(\ell)|\text{pos}(t) = m] = 0, \quad c \geq l \quad (62)$$

for any $m \in \{1, \dots, D\}$. For the case $c < l$, assume $\text{pos}(t) = m$ and $u, x \neq m$. The probability that the DD at positions u

and x is simultaneously modified when we remove a degree-one check node from m is

$$\xi_{m,u,x}(\ell) = \sum_{i=x-(l-1)}^u \lambda_{m,i}(\ell). \quad (63)$$

and, therefore,

$$\mathbb{E}[\Delta R_{j,u}(\ell) \Delta R_{z,x}(\ell) | \text{pos}(t) = m] = \quad (64)$$

$$jz \xi_{m,u,x}(\ell) \left(\frac{R_{j+1,u}(\ell) - R_{j,u}(\ell)}{\sum_{q=1}^r R_{q,u}(\ell)} \right) \left(\frac{R_{z+1,x}(\ell) - R_{z,x}(\ell)}{\sum_{q=1}^r R_{q,x}(\ell)} \right)$$

for $u, x \neq m$, $c < l$ and $j, z < r$. For $j = r$ ($z = r$), we just remove from (64) the term in $j + 1$ ($z + 1$). Assume now that $\text{pos}(\ell) = x$ and $c < l$. We know the the graph at position x just losses a degree-one check node. Hence, for $j = 1, \dots, r$

$$\mathbb{E}[\Delta R_{j,u}(\ell) \Delta R_{z,x}(\ell) | \text{pos}(t) = x] = 0 \quad (65)$$

for $z \geq 2$ and, for $z = 1$,

$$\mathbb{E}[\Delta R_{j,u}(\ell) \Delta R_{1,x}(\ell) | \text{pos}(t) = x]$$

$$= -j \xi_{x,u}(\ell) \frac{R_{j+1,u}(\ell) - R_{j,u}(\ell)}{\sum_{q=1}^r R_{q,u}(\ell)}, \quad (66)$$

where for $j = r$ $R_{j+1,u}(\ell)$ is zero. On the variable side, the expectation

$$\mathbb{E}[\Delta V_u(\ell) \Delta V_x(\ell)] = 0 \quad (67)$$

$u \neq x$ since the variable profile is only modified in one position per iteration. Consider now the moments of the form

$$\mathbb{E}[\Delta R_{j,u}(\ell) \Delta V_x(\ell)]. \quad (68)$$

Clearly, since a variable at position $x = u + c$ is connected to check nodes at positions $x, \dots, x + (l - 1)$, (68) is zero for $c \geq l$. For $c < l$, then the variable node at x is connected to a check at position u with probability one. Therefore,

$$\mathbb{E}[\Delta R_{j,u}(\ell) \Delta V_x(\ell) | \text{pos}(\ell) = m]$$

$$= -j \lambda_{m,x}(\ell) \frac{R_{j+1,u}(\ell) - R_{j,u}(\ell)}{\sum_{q=1}^r R_{q,u}(\ell)} \quad (69)$$

for $u \neq m$. For $\text{pos}(\ell) = u$, the DD at position u losses one degree one check node with probability one and thus

$$\mathbb{E}[\Delta R_{j,u}(\ell) \Delta V_x(\ell) | \text{pos}(\ell) = u] = \lambda_{u,x}(\ell) \quad (70)$$

for $j = 1$ and zero for $j \neq 1$.

2) *Same positions. Case $x = u$:* Our goal now is to compute moments of the form

$$\mathbb{E}[\Delta R_{j,u}(\ell) \Delta R_{z,u}(\ell)] \quad (71)$$

for any position u and degrees j and z . The procedure is similar to that followed in Section A. Assume we remove a degree-one check node placed at position $m \neq u$. A check node at position u losses one edge with probability $\xi_{m,u}(\ell)$. With probability

$$\frac{R_{j,u}(\ell)}{\sum_{q=1}^r R_{q,u}(\ell)} \quad (72)$$

the check node is of degree j . In this case, we loose j edges of right degree j and we win $j - 1$ edges with right degree $j - 1$. The rest of the DD terms are not affected. Therefore, for $|z - j| \geq 2$,

$$\mathbb{E}[\Delta R_{j,u}(\ell) \Delta R_{z,u}(\ell) | \text{pos}(\ell) = m] = 0, \quad (73)$$

for $z = j + 1$ we get

$$\mathbb{E}[\Delta R_{j,u}(\ell) \Delta R_{j+1,u}(\ell) | \text{pos}(\ell) = m]$$

$$= -j(j - 1) \xi_{m,u}(\ell) \frac{R_{j+1,u}(\ell)}{\sum_{u=1}^r R_{q,u}(\ell)}, \quad (74)$$

and for $j = z$

$$\mathbb{E}[\Delta R_{j,u}(\ell)^2 | \text{pos}(\ell) = m] =$$

$$j^2 \xi_{m,u}(\ell) \frac{R_{j+1,u}(\ell) + R_{j,u}(\ell)}{\sum_{u=1}^r R_{q,u}(\ell)}. \quad (75)$$

for $j \in \{1, \dots, r - 1\}$. For $j = r$, (74) is equal to zero. Finally, for $\text{pos}(\ell) = u$, (73) is zero except for the case $z = j = 1$:

$$\mathbb{E}[\Delta R_{1,u}(\ell)^2 | \text{pos}(\ell) = u] = 1. \quad (76)$$

On the variable side, it is straightforward to compute

$$\mathbb{E}[\Delta R_{j,u}(\ell) \Delta V_u(\ell) | \text{pos}(\ell) = m]$$

$$= -j \lambda_{m,u}(\ell) \frac{R_{j+1,u}(\ell) - R_{j,u}(\ell)}{\sum_{q=1}^r R_{q,u}(\ell)}, \quad (77)$$

for $j = 1, \dots, r - 1$. For $j = r$ we remove the term $R_{j+1,u}(\ell)$ from the equation above. And, finally

$$\mathbb{E}[\Delta^2 V_u(\ell) | \text{pos}(\ell) = m] = \lambda_{m,u}(\ell). \quad (78)$$

for $u = \{1, \dots, D\}$.

APPENDIX C

COVARIANCE INITIAL CONDITIONS

In Section III-B, we computed the expected DD after the PD initialization step. We are now interested in covariance moments between different components in $\mathcal{G}(0)$. Consider a position u in the range $[l, \dots, L]$, where all check nodes of the ensemble (l, r, L) are of degree r . After PD initialization, the degree of the check nodes at position u is distributed according to a Multinomial distribution with $\frac{l}{r}M$ trials and probabilities

$$p_{j,u} = \binom{r}{j} \epsilon^j (1 - \epsilon)^{r-j} \quad (79)$$

for $j = 0, \dots, r$. Therefore,

$$\text{Var}[R_{j,u}(0)] = j^2 \frac{l}{r} M p_{j,u} (1 - p_{j,u}), \quad (80)$$

$$\text{CoVar}[R_{j,u}(0), R_{z,u}(0)] = -jz \frac{l}{r} M p_{j,u} p_{z,u}. \quad (81)$$

Besides, variable nodes are independently removed and therefore

$$\text{Var}[V_u(0)] = M \epsilon (1 - \epsilon), \quad (82)$$

$$\text{CoVar}[V_u(0), V_x(0)] = 0 \quad u \neq x. \quad (83)$$

Let us now detail the computation of moments of the form

$$\text{CoVar}[R_{j,u}(0), R_{z,x}(0)] \quad (84)$$

for $x \neq u$. First, if positions u and x are separated l sections or further, there are no variable nodes connected check nodes to both sections and thus (84) is zero for any pair (j, z) . Consider the case $x = u + c$ where $c < l$. In this case, in the ensemble (l, r, L) there are $l - c$ positions, from position $x - l + 1$ to position u , that contain variable nodes connected to check nodes at positions u and x . Consider a pair of check nodes N_u and N_x selected at random from positions u and x . Let a (b) be the number of edges of N_u (N_x) that are connected to variable nodes at positions in the range $\{x - l + 1, \dots, u\}$. Both a and b are independent random variables that are distributed according to a Binomial distribution with number of trials r and probability $(c - l)/l$. For a given pair (a, b) , the probability that N_u and N_x are connected to the same variable node is simply given by

$$(l - c) \frac{ab}{M}. \quad (85)$$

By averaging (85) over all possible pairs (a, b) we can compute the probability that N_u and N_x share one variable node:

$$P_S = \frac{l - c}{M} r^2 \left(\frac{l - c}{l} \right)^2. \quad (86)$$

In the following, we neglect the case that N_u and N_x share two variable nodes since the probability of this to happen decays by M^{-2} . Denote by d_u and d_x the degree of the check nodes N_u and N_x respectively after initialization. The joint probability mass function of each pair (d_u, d_x) can be expressed as follows:

$$P(d_u = j, d_x = z) = P(d_u = j, d_x = z | \text{share}) P_S + P(d_u = j, d_x = z | \text{no share}) (1 - P_S), \quad (87)$$

where $P(d_u = j, d_x = z | \text{share})$ represents the joint probability distribution of the degrees d_j and d_x for the case where check nodes N_u and N_x share one variable node. It is straightforward to show that

$$P(d_u = j, d_x = z | \text{share}) \quad (88) \\ = \epsilon \left[\binom{r-1}{j-1} \epsilon^{j-1} (1-\epsilon)^{r-j} \binom{r-1}{z-1} \epsilon^{z-1} (1-\epsilon)^{r-z} \right] \\ + (1-\epsilon) \left[\binom{r-1}{j} \epsilon^j (1-\epsilon)^{r-j-1} \binom{r-1}{z} \epsilon^z (1-\epsilon)^{r-z-1} \right],$$

and

$$P(d_u = j, d_x = z | \text{no share}) = p_{j,u} p_{z,x}, \quad (89)$$

where $p_{j,u}$ and $p_{z,x}$ are given in (79). Using these expressions and averaging over all possible (N_u, N_x) pairs (there are $(l/rM)^2$ pairs in total), we obtain:

$$\text{CoVar}[R_{j,u}(0), R_{z,x=u+c}(0)] = jzM(l-c)^3 \quad (90) \\ \times \left(P(d_u = j, d_x = z | \text{share}) - P(d_u = j, d_x = z | \text{no share}) \right)$$

for $u, x \in [l, \dots, L]$, $j, z \in [1, \dots, r]$ and $c < l$. By following a similar procedure, we obtain

$$\text{CoVar}[V_u(0), R_{j,x=u+c}(0)] \\ = jM\epsilon^j (1-\epsilon)^{r-j} \left[\binom{r-1}{j-1} - \binom{r}{j} \epsilon \right] \quad (91)$$

for $u, x \in [l, \dots, L]$ and $c < l$. For $c \geq l$, the covariance in (91) is zero since the DDs at positions u and $x = u + c$ are independent. In this Appendix, we have restricted the computations of covariance moments of the DD $\mathcal{G}(0)$ involving positions in the (l, r, L) ensemble where the check degree is constant to r . The covariance moments relating positions $[1, \dots, l - 1]$ or $[L + 1, \dots, L + l - 1]$ can be computed in a similar way.